

Chapter 8: Modeling molecular diffusion

Computational Methods in Molecular and Cellular Biology: from Genotype to Phenotype.

J.M. Bower and H. Bolouri editors

MIT Press, Boston Reviews in the Neurosciences

G.Bormann¹, F. Brosens², [E. De Schutter](#)¹

1. *Born-Bunge Foundation, University of Antwerp - UIA, B2610 Antwerp, Belgium*

2. *Dept. of Physics, University of Antwerp - UIA, B2610 Antwerp, Belgium*

1. Introduction

1.1 Why model diffusion in cells?

Physical proximity is an essential requirement for molecular interaction to occur, whether it is between an enzyme and its substrate and modulators or between a receptor and its ligand. Cells have developed many mechanisms to bring molecules together, including structural ones, e.g. calcium-activated ionic channels often cluster with calcium channels in the plasma membrane (Gola and Crest, 1993; Issa and Hudspeth, 1994), or specific processes like active transport (Nixon, 1998). In many situations, however, concentration gradients exist which will affect the local rate of chemical reactions. Such gradients can be static at the timescale of interest, e.g. the polarity of cells (Kasai and Petersen, 1994), or very dynamic like for example the intra- and intercellular signaling by traveling calcium waves (Berridge, 1997).

Diffusion is the process by which random Brownian movement of molecules or ions cause an average movement towards regions of lower concentration, which may result in the collapse of the concentration gradient. In the context of cellular models, one distinguishes-experimentally and functionally-between free diffusion and diffusion across or inside cell membranes (Hille, 1992). We will only consider the first case explicitly, but similar methods as described here can be applied to the latter.

Historically, diffusion has often been neglected in molecular simulations which are then assumed to operate in 'the well-mixed pool'. This assumption may be valid when modeling small volumes, e.g. inside a spine (Koch and Zador, 1993), but should be carefully evaluated in all other contexts. As we will see in this chapter, the introduction of diffusion into a model raises many issues which otherwise do not apply: spatial scale, dimensionality, geometry and which individual molecules or ions can be considered to be immobile or not. The need for modeling diffusion should be evaluated for each substance separately. In general, if concentration gradients exist within the spatial scale of interest it is highly likely that diffusion will have an impact on the modeling results, unless the gradients change so slowly that they can be considered stationary compared to the timescale of interest. Simulating diffusion is in general a computationally expensive decision which is a more practical explanation of why it is often not implemented. This may very well change in the near future. A growing number of modeling studies (Markram *et al.*, 1998; Naraghi and Neher, 1997) have recently

emphasised the important effects diffusion can have on molecular interactions.

1.2 When is diffusion likely to make a difference?

A reaction-diffusion system is classically described as one where binding reactions are fast enough to affect the diffusion rate of the molecule or ion of interest (Wagner and Keizer, 1994; Zador and Koch, 1994). A classic example which we will consider is the interaction of calcium with intracellular buffers, which cause calcium ions to spread ten times slower than one would expect from the calcium diffusion constant (Kasai and Petersen, 1994).

Depending on which region of the cell one wants to model, this slow effective diffusion can be good or bad news. In fact, the slow effective diffusion rate will dampen rapid changes caused by calcium influx through a plasma membrane so much that in the center of the cell it can be modeled as a slowly changing concentration without gradient. Conversely, below the plasma membrane the slower changes in concentration gradient may need to be taken into full account (fig.3C).

This is, however, a static analysis of the problem while the dynamics of the reaction-diffusion process may be much more relevant to the domain of molecular interactions. In effect, as we will discuss in some detail, binding sites with different affinities may compete for the diffusing molecule which leads to highly nonlinear dynamics. This may be a way for cells to spatially organise chemical reactions in a deceptively homogenous intracellular environment (Markram *et al.*, 1998; Naraghi and Neher, 1997).

Before dealing with reaction-diffusion systems, however, we will consider the diffusion process itself in some detail. In this context we will consider especially those conditions under which the standard one-dimensional diffusion equation description used in most models is expected to fail.

2 Characteristics of diffusion systems.

Part I provided a concise introduction to the modeling of chemical kinetics based on mass action, expressed as reaction rate equations. It also discussed the shortcomings of the rate equation approach for describing certain features of chemical reactions and provided alternatives, e.g. Markov processes, to improve models of chemical kinetics.

These improvements stem from the realisation that under certain circumstances the stochastic nature of molecular interactions can have a profound effect on the dynamical properties. The resulting models still share a common assumption with rate equation models in that they assume a well-mixed homogenous system of interacting molecules. This ignores the fact that spatial fluctuations may introduce yet another influence on the dynamics of the system. For example, in many cases it is important to know how a spatially localised disturbance can propagate in the system. From statistical mechanics it follows that adding spatial dependence to the molecule distributions calls for a transport mechanism which dissipates gradients in the distribution. This mechanism is called diffusion and it is of a statistical nature. The effects on the dynamics of the chemical system are

determined by the relative timescales of the diffusion process and the chemical kinetics involved.

At the end of this section we will describe a number of examples of how diffusion interacts with a chemical system thereby creating new dynamics. First, however, we will consider diffusion by itself as an important and relatively fast transport mechanism in certain systems. We will also discuss how to relate diffusion to experimental data and show that such data mostly provide a warped view on diffusion. Therefore it is usually more appropriate to talk about 'apparent diffusion'. The appearance of this apparent diffusion, i.e. the degree of warpedness compared to free diffusion, is determined both by the nature of the chemical reactions and by the specific spatial geometry of the system under investigation.

This chapter provides methods of different nature to solve the equations that govern these phenomena and will give guidelines concerning their applicability. This should enable the reader to make initial guesses about the importance of diffusion in the system under consideration, which can help decide whether or not to pursue a more detailed study of the full reaction-diffusion system.

2.1 What is diffusion?

Diffusional behaviour is based on the assumption that the molecules perform a random walk in the space that is available to them. This is called Brownian motion. The nature of this random walk is such that the molecules have equal chance to go either way (in the absence of external fields). To see how this can generate a macroscopic effect (as described by Fick's law, see later) let's consider a volume element in which there are more molecules than in a neighbouring volume element. Although the molecules in both volume elements have equal chance of going either way, there are more molecules that happen to go to the element with the low initial number of molecules than there are molecules coming to the high initial number element because they simply outnumber them.

To describe this process mathematically we assume the molecules perform a discrete random walk by forcing them to take a step of fixed length Δx in a random direction (i.e. left or right) every fixed Δt , independent of previous steps. The average change in number of molecules Δn_i^k at discrete position i in a timestep Δt from t_k to t_{k+1} for a high enough number of molecules is then given by (see for instance (Schulman, 1981))

$$n_i^{k+1} - n_i^k = \Delta n_i^k = p_l n_{i+1}^k - (p_l + p_r) n_i^k + p_r n_{i-1}^k \quad (1)$$

where p_l and p_r are the probabilities to go either to the left or to the right. In the absence of drift we have for the probabilities (using the sum rule for independent events)

$$\begin{cases} p_l + p_r & = & 1 \\ p_l & = & p_r \end{cases} \quad (2)$$

so that $p_f = p_r = 1/2$

Filling in these numbers in eq.(1) gives

$$\begin{aligned}\Delta n_j^k &= \frac{1}{2}n_{j+1}^k - n_j^k + \frac{1}{2}n_{j-1}^k \\ &= \frac{1}{2}(n_{j+1}^k - 2n_j^k + n_{j-1}^k) \\ &= \frac{\Delta x^2}{2} \frac{n_{j+1}^k - 2n_j^k + n_{j-1}^k}{\Delta x^2}\end{aligned}\quad (3)$$

resulting in

$$\frac{\Delta n_j^k}{\Delta t} = \frac{\Delta x^2}{2\Delta t} \frac{n_{j+1}^k - 2n_j^k + n_{j-1}^k}{\Delta x^2}\quad (4)$$

Letting $\Delta x \rightarrow 0$ and $\Delta t \rightarrow 0$ while keeping

$$D = \frac{(\Delta x)^2}{2\Delta t}\quad (5)$$

constant (and multiplying both sides with a constant involving Avogadro's number ($6.022 \cdot 10^{23} \text{ mol}^{-1}$) and volume to convert to concentrations), we get the following parabolic PDE: [1]

$$\frac{\partial C(x,t)}{\partial t} = D \frac{\partial^2 C(x,t)}{\partial x^2}\quad (6)$$

This is generally known as the one-dimensional diffusion equation along a Cartesian axis. Other one-dimensional equations are used more often but they arise from symmetries in a multi-dimensional formulation, e.g. the radial component in a spherical or cylindrical coordinate system (see below). The random walk can be easily extended to more dimensions by using the same update scheme for every additional (Cartesian) coordinate.

The random walk process described above generates a Gaussian distribution of molecules over all grid positions when all molecules start from a single grid position x_0 (i.e. a Dirac delta function) :

$$C(x,t) = \frac{C_0}{\sqrt{4\pi Dt}} \exp\left(-\frac{(x-x_0)^2}{4Dt}\right)\quad (7)$$

It's left as an exercise for the reader to [proof this \[2\]](#). From this, and the fact that every function can be written as a series of delta functions, it follows that the same solution can be generated using a continuous random walk by drawing the step size each molecule moves every timestep Δt from a Gaussian of the form

$$N_{\Delta t}(\Delta x) = \frac{1}{\sqrt{4\pi D\Delta t}} \exp\left(-\frac{(\Delta x)^2}{4D\Delta t}\right) \quad (8)$$

which has a mean square step size of $(\Delta x)^2 = 2D \Delta t$, relating the two random walk methods. The choice of the method to use is determined by the following : discrete random walks allow a fast evaluation of the local density of molecules while continuous random walks allow easy inclusion [\[3\]](#) of complex boundary conditions.

The above is a quick way to determine the solution of eq.(6) for the initial condition [\[4\]](#) $C(x,0) = C_0 \delta(x-x_0)$. This is one of the few cases that can also be solved analytically. See Crank (Crank, 1975) for a general and extensive analytical treatment of the diffusion equation.

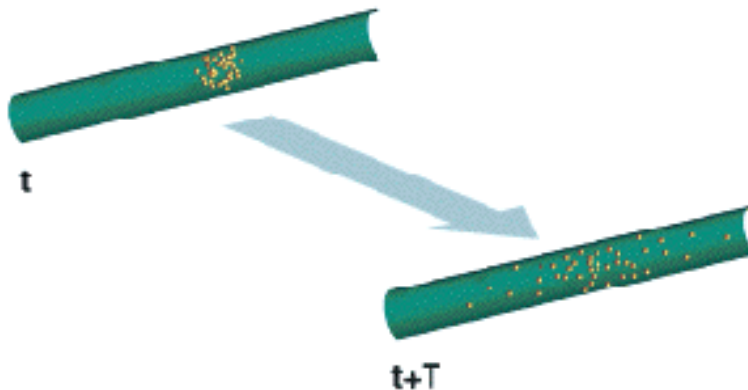


Figure 1

The initial condition is the distribution of molecules on a fixed time t (chosen as $t=0$ in most cases). It determines the final shape of the distribution at a later time $t+T$. In general, a partial differential equation (in space and time) has a set of possible solutions for a fixed set of parameters and (spatial) boundary conditions. By setting the initial condition, one selects a specific solution.

A final remark concerning the scale on which the random walk approach applies should be made. The movements the molecules make in the diffusion process are related to the thermal movement of and collisions with the background solvent molecules. The path a single molecule follows is erratic but each step is deterministic when the molecules are considered to be hard spheres. If the environment of the molecule is random though, the resulting path can be considered the result of a random walk where each step is independent of the molecule's history(Hille, 1992).

Nevertheless, even in a fluid the close range environment of a molecule has some short term symmetry in the arrangement of the surrounding molecules

so that on the scale of the mean free path (and the corresponding pico/femto second time scale) there is some correlation in the steps of the molecule-i.e. the molecule appears to be trapped in its environment for a short time. At this scale using random walks is not appropriate and one has to resort to Molecular Dynamics instead. At a larger distance (and thus at a longer timescale), the environment appears random again in a fluid and the correlations disappear so that a random walk approach is valid again.

2.2 A macroscopic description of diffusion.

Many discussions about diffusion start out with an empirical law : Fick's law (Fick, 1885). This law states that a concentration gradient for a dissolved substance gives rise to a flux of mass in the (diluted) solution, proportional to but in the opposite direction of the concentration gradient. The constant of proportionality is called the (macroscopic) diffusion constant. It is valid under quite general assumptions. The corresponding equation in one dimension is of the form

$$J_F(x,t) = -D \frac{\partial C(x,t)}{\partial x} \quad (9)$$

where D is the macroscopic diffusion constant and C(x,t) is the mass distribution function expressed as a concentration. The minus sign is there to ensure that the mass will flow downhill on the concentration gradient (otherwise we get an unstable system and the thermodynamic law of entropy would be violated).

The diffusion constant is usually treated as a fundamental constant of nature for the species at hand, determined from diffusion experiments. It is, however, not a real fundamental constant since it can be calculated, using kinetic gas theory, from thermodynamic constants, absolute temperature and molecule parameters. In fact, it can even be position-dependent if the properties of the medium (like the viscosity) vary strongly with position. So, including diffusion in an accurate model could become a messy business in some cases.

Fick's law looks very much like an expression for a flux proportional to a conservative force on the molecules, with the 'force' depending on the gradient of a field potential (the concentration). But, as can be concluded from section 5, that 'force' is entirely of a statistical nature. The flux of mass changes the concentration at all points of nonzero net flux. The rate of change is given by a mass balance (i.e. a continuity) equation as follows

$$\frac{\partial C(x,t)}{\partial t} = - \frac{\partial J_F(x,t)}{\partial x} \quad (10)$$

in the absence of other nonFickian fluxes. Replacing $J_F(x,t)$ by the right-hand side of eq.(9) gives eq.(4) if we identify the diffusion constant with the former

constant D . For more details on kinetic gas theory and a derivation of this macroscopic diffusion constant from microscopic considerations, see for example *The Feynman Lectures* (Feynman *et al.*, 1989). A classic is of course Einstein's original treatment of Brownian motion (Einstein, 1905). Eqs.(9) and (10) can be easily extended to higher dimensions by using the following vector notations

$$\begin{cases} \vec{J}_r(\vec{r}, t) &= -D\vec{\nabla}C(\vec{r}, t) \\ \frac{\partial C(\vec{r}, t)}{\partial t} &= -\vec{\nabla} \cdot \vec{J}_r(\vec{r}, t) \end{cases} \quad (11)$$

where " $\vec{\nabla}$ " is the gradient operator and " $\vec{\nabla} \cdot$ " the divergence operator. Combining the two equations then gives the general multi-dimensional diffusion equation

$$\frac{\partial C(\vec{r}, t)}{\partial t} = D\nabla^2 C(\vec{r}, t) = D\Delta C(\vec{r}, t) \quad (12)$$

with Δ the Laplace operator (Laplacian). The explicit form of the Laplacian depends on the chosen coordinate system. In a Cartesian system in ordinary space it looks like this

$$\frac{\partial C(x, t)}{\partial t} = -\frac{\partial J_r(x, t)}{\partial x} \quad (13)$$

Sometimes the nature of the problem is such that it is simpler to state the problem in cylindrical [5]

$$\Delta C(\rho, \phi, z, t) = \left(\frac{1}{\rho} \frac{\partial}{\partial \rho} \left(\rho \frac{\partial}{\partial \rho} \right) + \frac{1}{\rho^2} \frac{\partial^2}{\partial \phi^2} + \frac{\partial^2}{\partial z^2} \right) C(\rho, \phi, z, t) \quad (14)$$

or spherical [6] coordinates

$$\Delta C(r, \theta, \phi, t) = \left(\frac{1}{r} \frac{\partial^2}{\partial r^2} (r \cdot) + \frac{1}{r^2 \sin \theta} \frac{\partial}{\partial \theta} \left(\sin \theta \frac{\partial}{\partial \theta} \right) + \frac{1}{r^2 \sin^2 \theta} \frac{\partial^2}{\partial \phi^2} \right) C(r, \theta, \phi, t) \quad (15)$$

In case of axial respectively. spherical symmetry this reduces to the following more generally used (one-dimensional) radial equations

$$\begin{cases} \frac{\partial C(\rho,t)}{\partial t} = \frac{D}{\rho} \frac{\partial}{\partial \rho} \left(\rho \frac{\partial C(\rho,t)}{\partial \rho} \right) = D \frac{\partial^2 C(\rho,t)}{\partial \rho^2} + \frac{D}{\rho} \frac{\partial C(\rho,t)}{\partial \rho} \\ \frac{\partial C(r,t)}{\partial t} = \frac{D}{r} \frac{\partial^2 (rC(r,t))}{\partial r^2} = D \frac{\partial^2 C(r,t)}{\partial r^2} + \frac{2D}{r} \frac{\partial C(r,t)}{\partial r} \end{cases} \quad (16)$$

The solution of the spherical radial equation for an instantaneous point source, i.e. for an initial condition of the form $C(r,0)=C_0 \delta(r)/r$, is (for $r_0=0$)

$$C(r,t) = \frac{C_0}{2Dt} \exp\left\{-\frac{r^2}{4Dt}\right\} \quad (17)$$

This is the radial equivalent of eq.(7) and again this is actually one of the few solutions that can be found analytically. Both solutions describe one-dimensional diffusion in an infinite space and especially the last one is generally referred to as free diffusion.

2.3 Importance of boundary conditions and dimensionality.

Often, properties of diffusion are derived from free diffusion, following eq. (6), and proposed as generic diffusion properties while the actual boundary conditions shape the concentration profiles in significantly different ways. Knowing these shapes can be important when interpreting experimental results or when selecting curves-i.e. solutions of model problems-for fitting experimental data to estimate (apparent) diffusion parameters.

Choosing the appropriate boundary conditions is also important from a modeling point of view. Free diffusion is of use to model interactions in infinite space or in a bulk volume on appropriate timescales, i.e. situations where diffusion is used as a simple passive transport or dissipative mechanism. However, when diffusion is used as a transport mechanism to link cascading processes that are spatially separated or when diffusion is used in conjunction with processes that are triggered at certain concentration level thresholds, a detailed description of the geometry of the system may become very important. In that case the complex geometry can impose the majority of the boundary conditions.

To give an example, let's consider a cylinder of infinite length, with a reflecting mantle, in which there is an instantaneous point source releasing a fixed amount of substance A while further down the cylinder there is a store of another substance B. The store starts releasing substance B when the concentration of substance A reaches a certain threshold level. For smaller radii of the cylinder the time of release from the store will be much shorter. This is because the concentration of A at the store will rise sooner to the threshold level for smaller radii, although the intrinsic diffusion rate of A does not change.

When the concentration level of A has to be sustained for a longer period,

consider what happens when we seal off the cylinder with a reflecting wall near the point source. Since mass can now only spread in one general direction, the concentration of A can become almost twice as high as compared to the unsealed case, the exact factor depending on the distance between the point source and the sealed end. Furthermore, the concentration near the store and point source will stay elevated for a longer period of time. Eventually, the concentration will drop to zero in this case since the cylinder is still semi-infinite. When we seal off the other end too (at a much larger distance), then the concentration of A will, not surprisingly, drop to a fixed rest level-above or below the threshold level, depending just on the volume of the now finite closed cylinder-when no removal processes are present.

Boundary conditions play also a major role in the dimensionality of the diffusion equation one has to choose. Eqs.(16) are examples of equations that arise from certain symmetries in the boundary conditions. Often the dimensionality is also reduced by neglecting asymmetries in some components of the boundary conditions or by averaging them out for these components in order to reduce computation time or computational complexity. In some cases, though, it is necessary to keep the full dimensionality of the problem to be able to give an accurate description of the system. This is for example the case in cell models where compartmentalization is obtained through spatial co-localization of related processes. In order to simulate such models, one has to resort to fast multi-dimensional numerical methods. The methods section provides two such methods: one finite differencing method called ADI and one Monte Carlo method called Green's Function Monte Carlo.

2.4 Interactions among molecules and with external fields.

In the reaction rate equation approach a system of chemical reactions can be described in general by a set of coupled first-order ODE's:

$$\left\{ \begin{array}{l} \frac{dC_1(t)}{dt} = f_1(C_1, C_2, \dots, C_N) \\ \frac{dC_2(t)}{dt} = f_2(C_1, C_2, \dots, C_N) \\ \vdots \\ \frac{dC_N(t)}{dt} = f_N(C_1, C_2, \dots, C_N) \end{array} \right. \quad (18)$$

where the form of the functions f_s are determined by the reaction constants and structures of the M chemical reaction channels. The functions f_s are generally nonlinear in the C_s 's. In case the reaction mechanisms and constants are known, one can use the following normal form for the f_s 's:

$$f_c(C_1, C_2, \dots, C_N) = \sum_{s=1}^N K_{s,c} \prod_{i=1}^N C_i^{v_{i,c}^s} \quad (19)$$

with $K_{s,c} = k_c(v_{s,c}^R - v_{s,c}^L)$, where the $(v_{s,c}^L, v_{s,c}^R)$ are the stoichiometric coefficients for substance s on the left-hand respectively right-hand side of the reaction equation for reaction c [7] and k_c is the reaction constant. Most

of the $v_{s,c}^L$ and/or $v_{s,c}^R$ are zero. $R_c = \sum_{i=1}^N v_{i,c}^L$ is known as the reaction order and is related to the order of the collisions between the reacting molecules. Since collisions of order higher than 4 are extremely improbable, $R_c \leq 4$ for most reactions. A reaction of higher order is most likely a chain of elementary reaction steps.

Combining the rate equations with a set of diffusion equations now results in a set of coupled nonlinear parabolic PDE's :

$$\begin{cases} \frac{\partial C_1(x, y, z, t)}{\partial t} = D_1 \Delta C_1(x, y, z, t) + f_1(C_1, C_2, \dots, C_N) \\ \frac{\partial C_2(x, y, z, t)}{\partial t} = D_2 \Delta C_2(x, y, z, t) + f_2(C_1, C_2, \dots, C_N) \\ \vdots \\ \frac{\partial C_N(x, y, z, t)}{\partial t} = D_N \Delta C_N(x, y, z, t) + f_N(C_1, C_2, \dots, C_N) \end{cases} \quad (20)$$

The first term of the right-hand side will be 0 for all immobile substances. Systems governed by a set of equations like eqs.(18) can exhibit a broad array of complex temporal patterns. Including a transport mechanism to introduce spatial dependence as described by eqs.(20) can introduce additional complex spatial patterns.

Only very simple cases can be solved analytically for both types of problems, so one has to resort to numerical methods which can become very involved for the second type of problems. At low molecule densities, classic integration methods like the ones introduced in section 14 cannot grasp the full dynamics of the system because they don't include the intrinsic fluctuations. One has to resort to stochastic approaches for the chemical kinetics like the ones introduced in Part I and for the diffusion like the Monte Carlo method introduced in the Numerical Methods section.

Reaction partners can be electrically charged. Although this can have an important influence on the reaction kinetics, it is usually handled by adjusting the rate constants (in case of rate models) or the reaction probabilities (in case of stochastic models). However, one can think of problems where it's important to know the effects of local or external electric

fields on diffusion. One can start studying these problems by rewriting eqs. (11) to

$$\begin{aligned}
 \vec{J}(\vec{r}, t) &= \vec{J}_p(\vec{r}, t) + \vec{J}_{ext}(\vec{r}, t) \\
 &= \vec{J}_p(\vec{r}, t) + \vec{J}_{ext}(\vec{r}, t) + \vec{J}_c(\vec{r}, t) \\
 &= -D \left(\vec{\nabla} C(\vec{r}, t) + \frac{zF}{RT} C(\vec{r}, t) \vec{\nabla} V \right) + \vec{J}_c(\vec{r}, t) \\
 \frac{\partial C(\vec{r}, t)}{\partial t} &= -\vec{\nabla} \cdot \vec{J}(\vec{r}, t) \\
 &= D \left(\Delta C(\vec{r}, t) + \frac{zF}{RT} \vec{\nabla} \cdot (C(\vec{r}, t) \vec{\nabla} V) \right) - \vec{\nabla} \cdot \vec{J}_c(\vec{r}, t)
 \end{aligned} \tag{21}$$

where \vec{J}_c is the net flux induced by the Coulomb interactions between the charged molecules and \vec{J}_{ext} the net flux induced by the interaction of the charged molecules with an external field of potential V . z is the valence of the ionic species, F is the Faraday constant, R is the gas constant and T is absolute temperature. The second equation is called the electrodiffusion

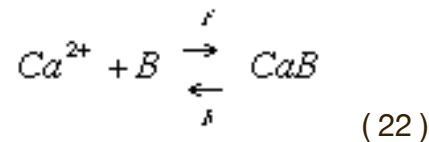
equation. In the case of $\vec{J}_c = 0$, it is called the Nernst-Planck equation (Hille, 1992). Special complicated numerical algorithms have to be used to solve the general electrodiffusion equation because of the long range and the $1/r$ divergence of Coulomb interactions. For an application to synaptic integration in dendritic spines, see for example Qian and Sejnowski (Qian and Sejnowski, 1990).

2.5 An example of reaction-diffusion systems: calcium buffering in the cytoplasm.

Reaction-diffusion systems have been studied most extensively in the context of buffering and binding of calcium ions. Calcium is probably the most important intracellular signaling molecule. Its resting concentration is quite low (about 50 nM) but it can raise by several orders of magnitude (up to 100's of μM 's) beneath the pore of calcium channels (Llinás *et al.*, 1992). Cells contain an impressive variety of molecules with calcium binding sites, this includes pumps which remove the calcium (e.g. the calcium-ATPase; (Garrahan and Rega, 1990)), buffers which bind the calcium (e.g. calbindin, calsequestrin, calretinin, etc.; (Baimbridge *et al.*, 1992)), enzymes activated by calcium (for example phospholipases; (Exton, 1997)) or modulated by calcium (for example through calmodulin activation; (Farnsworth *et al.*, 1995)). The interaction of the transient steep calcium concentration gradients with all these binding sites creates complex reaction-diffusion systems, the properties of which are not always completely understood. For example, it remains a point of discussion whether calcium waves, which are caused by inositol1,4,5-triphosphate (IP_3) activated release of calcium from intracellular

stores, propagate because of diffusion of IP_3 (Bezprozvanny, 1994; Sneyd *et al.*, 1995) itself or of calcium (Jafri and Keizer, 1995), which has a complex modulatory effect on the IP_3 receptor (Bezprozvanny *et al.*, 1991).

We will focus on the macroscopic interaction of calcium with buffer molecules. The main function of buffers is to keep the calcium concentration within physiological bounds by binding most of the free calcium. Almost all models of the interactions of calcium with buffers use the simple second-order equation:



Eq.(22) is only an approximation as most buffer molecules have multiple binding sites with different binding rates (Linse *et al.*, 1991) and require more complex reaction schemes (see first section of this book). In practice, however, experimental data for these different binding rates are often not available. Nevertheless, it is important to express buffer binding with rate equations, even simplified ones, instead of assuming the binding reactions to be in steady-state, described by the buffer dissociation constant $K_d=b/f$ like is often done (e.g. (Goldbeter *et al.*, 1990; Sneyd *et al.*, 1994)). Even if the time scale of interest would allow for equilibrium to occur, the use of steady-state equations neglects the important effects of the forward binding rate constant f on diffusion and competition between buffers (see further).

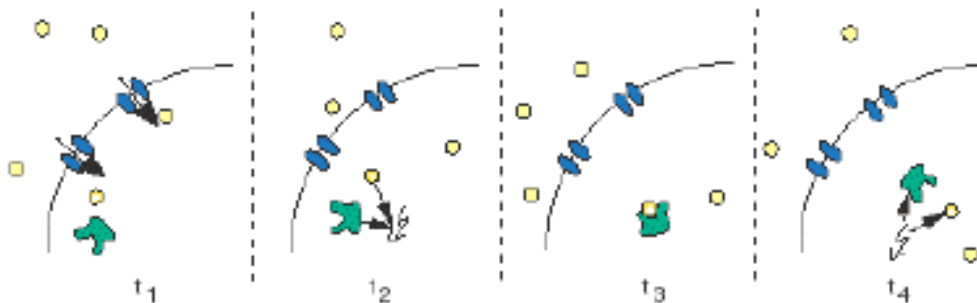


Figure 2

A pictorial description of the effect of buffer binding on calcium diffusion for slowly diffusing buffers. The yellow dots represent calcium ions, the green blobs buffer molecules, the purple blobs are calcium channels and the lightning symbol represents chemical interaction. The reacting dot is gradient-colored to distinguish it from the other intracellular dot. Note that the figure only shows the net effect for the respective populations. In reality, individual molecules follow erratic paths that don't directly show the buffering effect.

While the properties of buffered calcium diffusion have been mostly studied using analytical approaches (Naraghi and Neher, 1997; Wagner and Keizer, 1994; Zador and Koch, 1994), it is fairly simple to demonstrate these concepts through simulation of the system corresponding to the set of differential equations described in the next section (see also (Nowycky and Pinter, 1993) for a similar analysis). The simulations of the simple models

that [8] we used were run with the GENESIS software (the simulation scripts can be downloaded from the Web <http://www.tnb.ua.ac.be/models/models.shtml>). For more information on simulating calcium diffusion with the GENESIS software (Bower and Beeman, 1995) we refer to De Schutter and Smolen (De Schutter and Smolen, 1998). We will focus on the transient behavior of the reaction-diffusion system, i.e. the response to a short pulsatile influx of calcium through the plasma membrane. Also, as we are interested mostly in molecular reactions we will stay in the nonsaturated regime $[Ca^{2+}] \ll K_d$ though of course interesting nonlinear effects can be obtained when some buffers start to saturate. Finally, for simplicity we do not include any calcium removal mechanisms (calcium pumps ;(Garrahan and Rega, 1990) and the Na^+Ca^{2+} exchanger ;(DiFrancesco and Noble, 1985)), though they are expected to have important additional effects by limiting the spread of the calcium transients (Markram *et al.*, 1998; Zador and Koch, 1994).

The diffusion constant of calcium (D_{Ca}) in water is $6 \cdot 10^{-6} \text{cm}^2 \text{s}^{-1}$. In cytoplasm, however, the measured diffusion constant is much lower because of the high viscosity of this medium. Albritton *et al.* (Albritton *et al.*, 1992) measured a D_{Ca} of $2.3 \cdot 10^{-6} \text{cm}^2 \text{s}^{-1}$ in cytoplasm and other ions and small molecules can be expected to be slowed down by the same factor. As shown in fig.3A, with this D_{Ca} calcium rises rapidly everywhere in a typical cell, with only a short delay of about 10 ms in the deepest regions. After the end of the calcium influx, the calcium concentration reaches equilibrium throughout the cell in less than 200 ms. Down to about $3.0 \mu\text{m}$ the peak calcium concentration is higher than the equilibrium one because influx rates are higher than the rate of removal by diffusion.

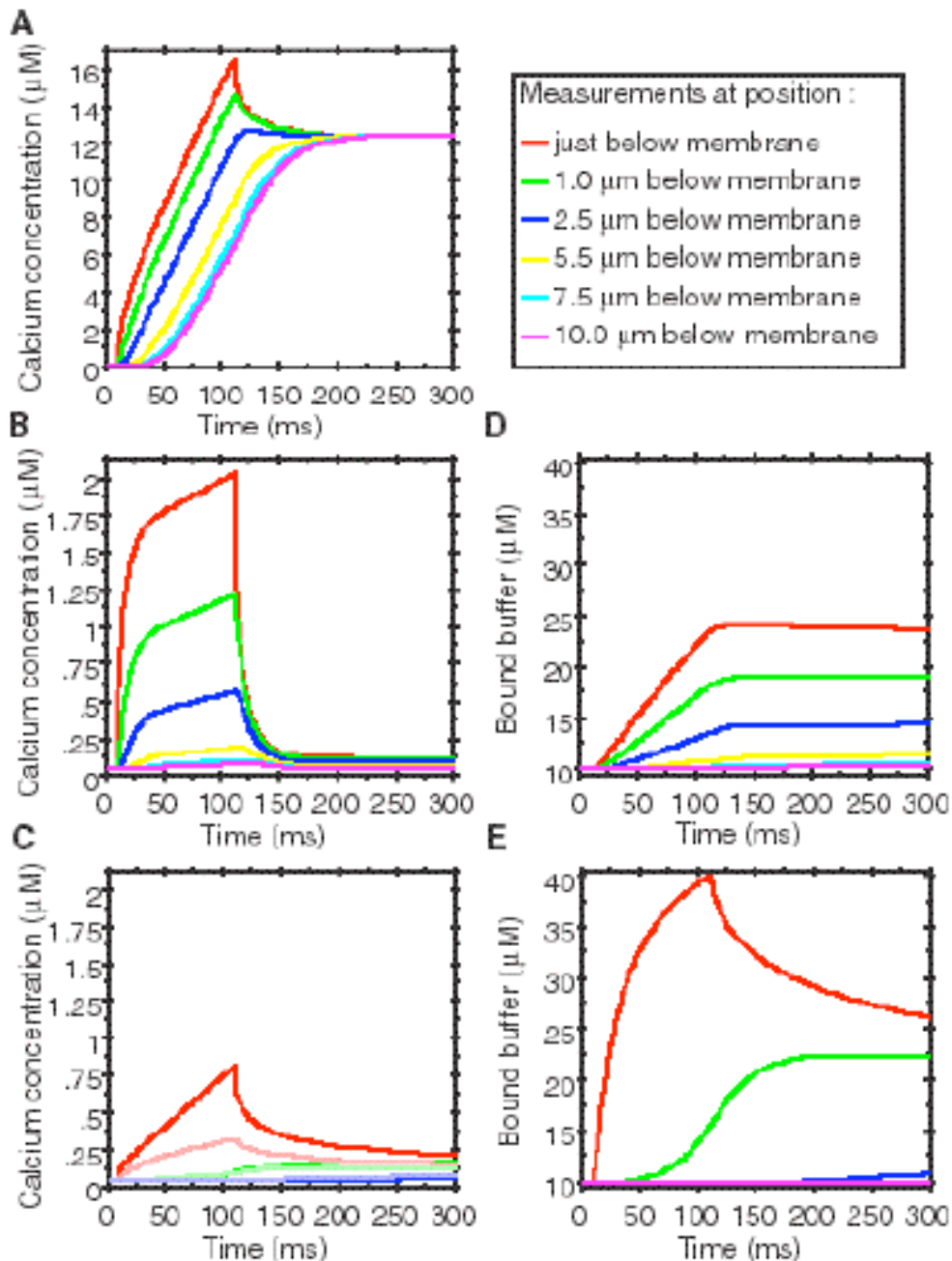


Figure 3

Effect of immobile buffer binding rates on calcium diffusion. The changes in calcium concentration at several distances from the plasma membrane) due to a short calcium current into a spherical cell are shown.

A Calcium concentration for simulation with no buffers present.

B Same with buffer with slow forward rate f (similar to EGTA) present.

C Same with buffer with fast f (similar to BAPTA) present. Fainter colors: approximation using D_{app} (eq.(24)).

D Bound buffer concentration for simulation shown in B

E Same for simulation shown in C

This diffusion constant is attained only if no binding to buffers occurs (Albritton *et al.*(Albritton *et al.*, 1992)) completely saturated the endogenous buffers with calcium to obtain their measurements). Figs.3(B-E)

demonstrates the effect of stationary buffers on the effective calcium diffusion rate: they decrease both the peak and equilibrium calcium concentration, slow the diffusion process down and limit the spread of calcium to the submembrane region (i.e. close to the site of influx). The total buffer concentration $[B]_T=[B]+[CaB]$ and its affinity, which is high in these simulations ($K_d=0.2 \mu M$), will determine the amount of free calcium at equilibrium. This is called the buffer capacity of the system, which is also the ratio of the inflowing ions that are bound to buffer to those that remain free (Augustine *et al.*, 1985; Wagner and Keizer, 1994) :

$$\kappa = \frac{d[CaB]_f}{d[Ca^{2+}]_f} = \frac{K_d[B]_f}{(K_d + [Ca^{2+}]_f)^2} \quad (23)$$

In case of low calcium concentration eq.(23) reduces to $[B]_T/K_d$. Buffer capacities in the cytoplasm are high, ranging from about 45 in adrenal chromaffin cells (Zhou and Neher, 1993) to more than 4000 in Purkinje cells (Llano *et al.*, 1994).

While the buffer capacity determines the steady-state properties of the system, the dynamics are highly dependent on the forward binding rate f (compare fig.3B with fig.3C). In effect, for the same amount of buffer and the same high affinity the calcium profiles are very different. For the slow buffer as in fig.3B, calcium rises rapidly everywhere in the cell with similar delays as in fig.3A, but reaches much lower peak concentrations. Only about 50% of the buffer gets bound below the plasma membrane. After the end of the calcium influx the decay to equilibrium has a very rapid phase, comparable to that in fig.3A, followed by a much slower relaxation which takes seconds. The peak calcium concentrations are comparatively much higher than the equilibrium concentration of 95 nM down to a depth of 5.0 μm . Note the slow relaxation to equilibrium of bound buffer in fig.3D Conversely, in the case of rapid binding buffer (fig.3C) calcium rises slowly below the plasma membrane, but does not start to rise 1.0 μm deeper until 50 ms later. Deeper, the calcium concentration does not start to rise until after the end of the calcium influx. Much more calcium gets bound to buffer (fig.3E) below the plasma membrane than in fig.3D. The decay to equilibrium is monotonic and slower than in fig.3A.

Both the differences during the influx and equilibration processes compared to the unbuffered diffusion are due to the binding and unbinding rates of the buffer, which dominate the dynamics. The buffer binding does not only determine the speed with which the transients rise, but also with which they extend toward deeper regions of the cell. This is often described as the effect of buffers on the apparent diffusion constant D_{app} of calcium (Wagner and Keizer, 1994):

$$D_{eff} \approx \frac{1}{1 + \kappa} D_{Ca} \quad (24)$$

This equation gives a reasonable approximation for distances sufficiently far from the source of influx, provided f is quite fast (Wagner and Keizer, 1994). For a fast buffer similar to BAPTA it does not capture the submembrane dynamics at all (fainter colors in fig.3C [9]). In conclusion, in presence of fast immobile buffers, experimental measurements of calcium diffusion can be orders of magnitude slower than in their absence. This severely limits the spatial extent to which calcium can affect chemical reactions in the cell compared to other signaling molecules with similar diffusion constants that are not being buffered, like IP_3 (Albritton *et al.*, 1992; Kasai and Petersen, 1994). Conversely, for the slower buffer (fig.3B) the initial dynamics (until about 50 ms after the end of the current injection) are mostly determined by the diffusion constant.

When the calcium influx has ended, the buffers again control the dynamics while the concentrations equilibrate throughout the cell. Because much more calcium is bound than free (buffer capacity of 250 in these simulations) the bulk of this equilibration process consists of shuffling of calcium ions from buffers in the submembrane region to those in deeper regions. As this requires unbinding of calcium from the more superficial buffer the dynamics are now dominated by the backward binding rate b , which is faster for the fast f buffer in fig.3C (both buffers having the same K_d). As a consequence the fast bound buffer concentration mimics the calcium concentration better than the slow bound buffer. This is an important point when choosing a fluorescent calcium indicator dye: the ones with fast (un)binding rates will be much more accurate (Regehr and Atluri, 1995). Finally, calcium removal mechanisms can also affect the equilibration process to a large degree: if the plasma membrane pumps remove the calcium ions fast enough they will never reach the lower regions of the cell, especially in the case of the buffer with fast f (where initially more calcium stays close to the plasma membrane).

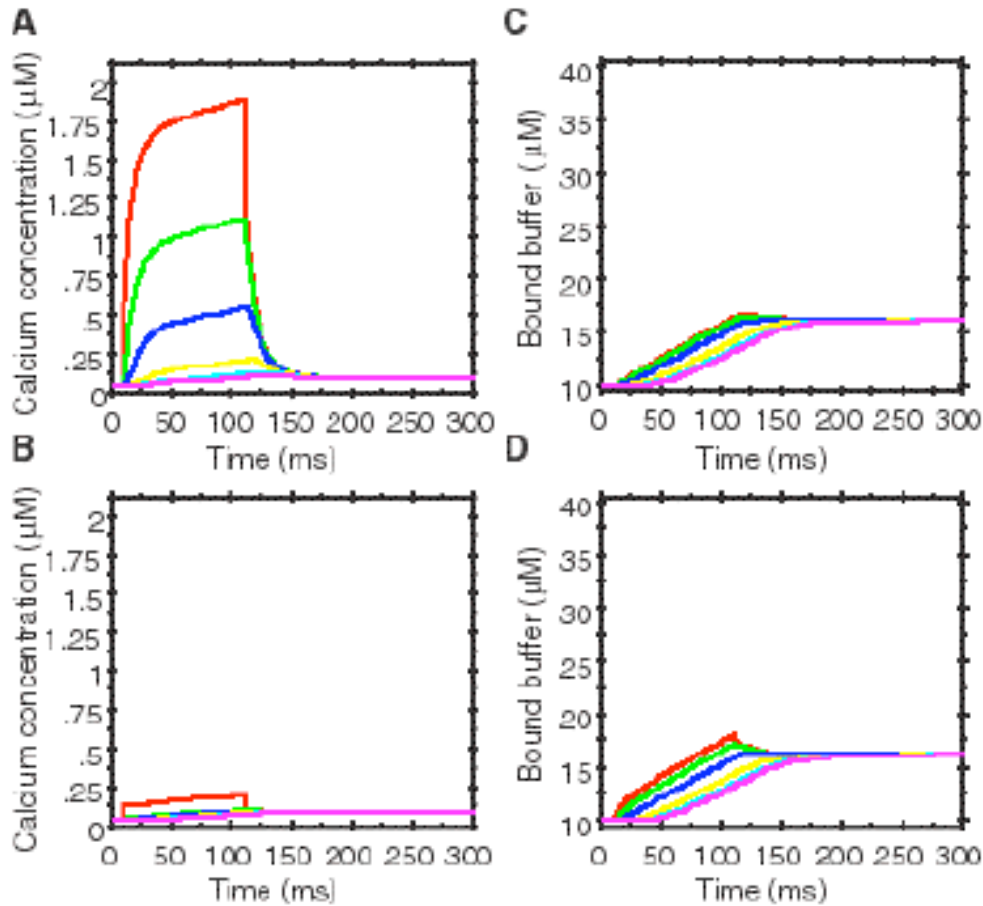


Figure 4

Effect of a diffusible buffer binding rates on calcium diffusion. Simulation results similar to those in Fig.3(B-E), but the buffer is now diffusible.

A Calcium concentration for simulation with diffusible buffer with slow forward binding rate f .

B Same with diffusible buffer with fast f .

C Bound buffer concentration for simulation shown in B

D Same for simulation shown in C

The above system changes completely when the buffer itself becomes diffusible (see schematic explanation in fig.2 and simulation results in fig.4). Now the buffer itself becomes a carrier for calcium ions: bound buffer diffuses to the regions of lower bound buffer concentration which simply are also regions of lower calcium concentration so that the bound buffer will unbind its calcium. Again this effect can be described by how the apparent diffusion constant D_{app} of calcium changes (Wagner and Keizer, 1994) :

$$D_{app} \approx \frac{1}{1 + \kappa} D_{Ca} + \kappa D_B \quad (25)$$

This equation has all the limitations of a steady-state approximation. It demonstrates, however, that diffusion of buffers (which in the case of ATP have D_B comparable to D_{Ca} in the cytoplasm; (Naraghi and Neher, 1997)) can compensate for the effect of (stationary) buffers on the apparent

diffusion rate. In the case of fig.4B, it does not capture the submembrane transient at all (not shown) but reproduces the transients at deeper locations well. The diffusive effect of mobile buffers is an important artifact that fluorescent calcium indicator dyes (e.g. fura-2) can introduce in experiments, because they will change the calcium dynamics themselves (Blumenfeld *et al.*, 1992; De Schutter and Smolen, 1998; Sala and Hernandez-Cruz, 1990). The actual effect on D_{app} , however, will depend again on the f rate of the buffer. In the case of a slow f rate the effect of buffer diffusion during the period of calcium influx are minor as the submembrane peak calcium concentration is only a bit lower compared to simulations with immobile buffer (compare fig.4A with fig.3B). At the same time the diffusible buffer saturates much less than the immobile one (fig.3C). The biggest difference is, however, after the end of the calcium influx: the system reaches equilibrium within 100 ms! Like in the case of immobile fast buffer (fig.3C), diffusible fast buffer (fig.4B) is much more effective in binding calcium than the slow one (compare to fig.4A), but even more so than the immobile one: now only the submembrane concentration shows a peak, at all other depths the concentrations increase linearly to equilibrium (and can be approximated well by eq.(25) for D_{app}) and this is reached almost immediately after the end of the calcium influx.

In general it is mainly during the equilibration period after the calcium influx that the buffer diffusion causes a very rapid spread of calcium to the deeper regions of the cell. In other words, the D_{app} will actually increase under these situations because the reaction-diffusion system moves from initially being dominated by the slow calcium diffusion (during influx D_{app} approaches D_{Ca}) to being dominated by the buffer diffusion (during equilibration where now only one unbinding step is needed instead of the shuffling needed with the immobile buffer). A similar phenomenon can be found in the case of longer periods of calcium influx: in this case the mobile buffer will start to saturate so that the unbinding process becomes more important and again D_{app} rises, but now during the influx itself (Wagner and Keizer, 1994).

When the buffer has a fast f rate the effects of buffer diffusion become more apparent during the calcium influx itself also (compare fig.4B with fig.3C)! One sees indeed an almost complete collapse of the calcium gradient because the buffer binds most of the calcium flowing into the submembrane region without being affected by saturation (it gets continuously replenished by free buffer diffusing upward from deeper regions of the cell).

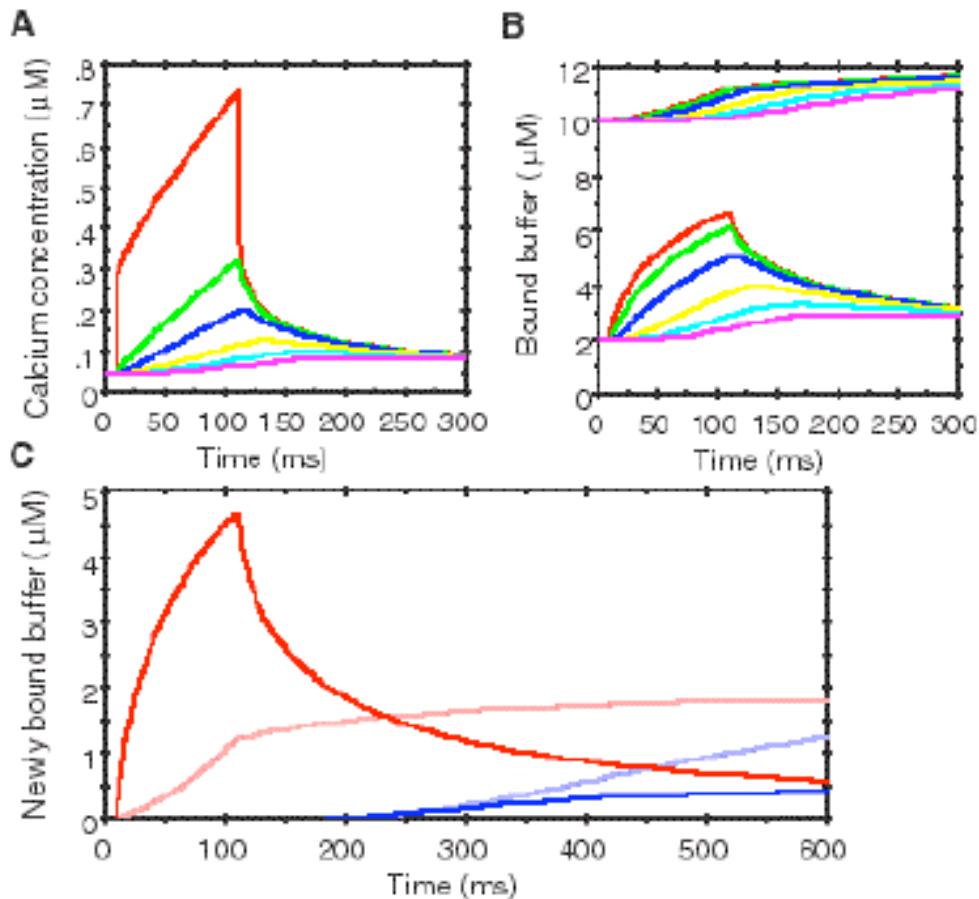


Figure 5

Effect of competition between two diffusible buffers. Simulations similar to those in Fig. 3(B-E), with both diffusible buffers present.

A Calcium concentrations.

B Bound buffer concentrations : upper traces slow buffer, lower traces fast buffer.

C Superposition of bound buffer traces for fast buffer and slow buffer (fainter colors; traces have been superimposed by subtracting the steady state bound buffer concentration). Concentrations just below the plasma membrane (red curves) and at 30 μm depth (blue curves) are shown.

We end this section with a consideration of how competition among buffers in a reaction-diffusion system can cause localization of binding reactions. This is demonstrated in fig.5 which shows a simulation where the same two buffers with identical affinities, but different homogenous concentrations, are present [10]. While the calcium concentrations (fig.5A) are somewhat similar to those in fig.4B, the peak concentrations are much smaller and the reaction-diffusion system takes a much longer time to reach equilibrium after the end of the calcium influx. More important are the large differences in the bound buffer profiles (fig.5B): the ones for the slow buffer rise continuously, while the ones for the fast buffer peak at low depths in the cell.

These differences are shown in more detail in fig.5C A peak in bound fast buffer concentration can be observed below the plasma membrane during the calcium influx: initially much more calcium is bound to the fast buffer than to the slow one (which has a five times higher concentration).

Conversely, in deeper regions of the cell, the slow buffer always dominates (fig.5C). This effect which has been called "relay race diffusion" by Naraghi and Neher (Naraghi and Neher, 1997) shows that, under conditions of continuous inflow, buffers have a characteristic length constant (depending on their binding rates, concentration and diffusion rate) which corresponds to the distance from the site of influx at which they will be most effective in binding calcium. If one replaces in the previous sentence the word buffer with calcium-activated molecule it becomes obvious that relay race diffusion can have profound effects on the signaling properties of calcium as it will preferentially activate different molecules depending on their distance from the influx or release site. The competition between buffers also slows down the dynamics of the reaction-diffusion system as calcium is again being shuttled between molecules (compare fig.4B and fig.5A).

Markram *et al.* (Markram *et al.*, 1998) have studied similar systems where calcium removal systems were included in the model. They show that if calcium removal is fast, only the fast binding molecules may be able to react with calcium ions during transients. Conversely, in a case of repetitive pulses of calcium influx, the slower binding molecules will keep increasing their saturation level during the entire sequence of pulses while the faster buffers will reach a steady saturation after only a few pulses (Markram *et al.*, 1998), demonstrating the sensitivity to temporal parameters of such a mixed calcium binding system. This is very reminiscent of recent experimental results demonstrating the sensitivity of gene expression systems to calcium spike frequency (Dolmetsch *et al.*, 1998; Li *et al.*, 1998).

3 Numerical Methods.

This section treats examples of two distinct classes of numerical methods to approximately solve the full reaction-diffusion system. The first class of methods tries to solve the set of reaction-diffusion equations by simulating the underlying chemical/physical stochastic processes and/or by integrating the equations using stochastic techniques. Because of their stochastic nature, they are generally referred to as Monte Carlo methods. The second class of methods tries to solve the set of reaction-diffusion equations directly by numerically integrating the equations. The methods are called the Crank-Nicholson method and the Alternating Direction Implicit (ADI) method.

3.1 Monte Carlo methods.

The term 'Monte Carlo method' is used for a wide range of very distinct methods that have one thing in common : they make use of the notion 'randomness' (through the use of computer-generated random numbers [11]), either to quickly scan a significant part of a multi-dimensional region or to simulate stochastic processes. The first type is used for efficiently integrating multi-variate integrals. Reaction-diffusion problems are more naturally solved [12] using the second type of MC methods. These MC methods can be subdivided once more in two classes : methods that follow the fate of individual molecules and methods that follow the fate of mass elements. We will give an introduction to the first class of methods, called

Diffusion MC, and work out in more details an example of the second class, called Green's Function MC.

3.2 Diffusion MC methods.

These methods use random walks to simulate the diffusional motion of every individual molecule. Successful applications include the study of synaptic transmission by simulating diffusion of neurotransmitter molecules across the synaptic cleft and including their reactions with postsynaptic receptors (Bartol *et al.*, 1991; Wahl *et al.*, 1996) and the study of G-protein activation in the submembrane region for a small membrane patch (Mahama and Linderman, 1994). Although their usefulness is proven, they suffer from two major problems.

The first problem is related to the inclusion of chemical reactions. These have to be simulated by detecting collisions between the walking molecules and current detection algorithms tend to be very inefficient. In addition, it is very hard to determine the reaction probabilities from the rate constants and/or molecule parameters since the molecule can experience more real, chemically effective, collisions than the random walk would allow for. Therefore these methods are only useful for simulating chemical reactions of mobile molecules with immobile ones on a surface, like receptors, so that one can use the notion of effective cross section to calculate the reaction probabilities.

The other problem is related to the scale of the system. Simulating individual molecules is only feasible for a small number of molecules, that is, on the order of ten thousand molecules [13] as is the case in the examples mentioned. If one is interested for instance in simulating a large part of a dendritic tree or when the concentration of a substance has a large dynamic range, as is the case for calcium, these methods will hit hard on computer memory usage and computation time.

A way to solve the first problem is to use a Molecular Dynamics (see Part I) approach which, however, suffers from the second problem as well, thereby eradicating the advantages of using random walks. A popular implementation of this kind of MC methods is MCell (Bartol *et al.*, 1996). The authors of Mcell pioneered the use of ray-tracing techniques for boundary detection in general MC simulators of biological systems.

3.3. Green's Function MC.

We introduce an MC method, that doesn't suffer from these problems as can be seen from the following. It's called Green's Function MC and it is based on a Quantum MC method from Solid State Physics (De Raedt and von der Linden, 1995). Technically, this method depends strongly on a result from function theory : every function can be expanded in a series of Dirac delta functions or

$$\bar{c}(\vec{r}, t_0) = \sum_{j=1}^{N_s} c_j(t_0) \delta(\vec{r} - \vec{r}_j) \quad (26)$$

where the $C_i(t_0) = C(\vec{r}_i, t_0)$ are $N \delta$ samples of the function $C(\vec{r}, t_0)$ at fixed points. In our case, it denotes the distribution function (expressed in concentration units for instance) of a substance at time t_0 . Finding the evolution of the function under an evolution equation boils down to finding the evolution of the coefficients $C_i(t_0 \rightarrow t)$. We know from section 5 that the solution of the diffusion equation for a Dirac delta function [14] is a Gaussian and that this Gaussian can be generated using a random walk, in this case a random walk in 3-space. In order to perform that random walk to solve the diffusion equation, we further subdivide the $C_i(t_0)$'s in n_i pieces of weight w_K and assign this weight to a random walker for every piece,

resulting in $N_w = \sum_{i=1}^{N_s} n_i$ walkers in total. Eq.(26) now becomes

$$\bar{C}(\vec{r}, t_0) = \sum_{i=1}^{N_s} \left(\sum_{k=1}^{n_i} w_k \right) \delta(\vec{r} - \vec{r}_i) \quad (27)$$

which is only valid for $t=t_0$ because at later times the successive random walk steps redistribute the walkers over neighboring positions so that we should write

$$\bar{C}(\vec{r}, t) = \sum_{i=1}^{N_s} \left(\sum_{k=1}^{n_i(t)} w_k \right) \delta(\vec{r} - \vec{r}_i) \quad (28)$$

instead for later times ($t > t_0$). $n_i(t)$ is the number of all walkers for which the position $\vec{r}_{*k} \in \Delta V_i$, ΔV_i being a neighborhood of \vec{r}_i and $\bigcup_{i=1}^{N_s} \Delta V_i = V$ ($\Delta V_i \cap \Delta V_{i_2} = \emptyset, i_1 \neq i_2$), the region in space in which the simulation takes place. When proper accounting of walkers is done, $N_w = R_i n_i(t)$ should be the initial number of walkers for every step. The easiest way to perform the random walk, however, is to divide all $C_i(t_0)$'s in n_i equal pieces of weight w . At time t , $C(\vec{r}, t)$ can now be approximated by

$$\bar{C}(\vec{r}, t) = w \sum_{i=1}^{N_s} n_i(t) \delta(\vec{r} - \vec{r}_i) \quad (29)$$

with $n_i(t)$ the number of walkers at or near. As a consequence, simulating diffusion has now become as simple as taking N_w samples of equal size w of the initial distribution function and keeping track of all the samples as they independently perform their random walks. In a closed region V , choose weights $w = (C_0 V) / N_w$ where C_0 is for example the final concentration at equilibrium and $V = \text{vol}(V)$. For pure diffusion, all mass that was present

initially will be preserved so that the weights stay unchanged. Note that N_w determines the variance of the fluctuations around the expected mean [15] and can be *much smaller* than the number of molecules present in V . Therefore this Green's Function MC method does *not* suffer from the same bad scaling properties as the diffusion MC methods. Implementing chemical interactions (in fact, almost any interaction) has now become straightforward. To make the idea clear while keeping it simple we will use a reaction-rate approach. Once this is understood, it shouldn't be too hard to switch to a population level description (as opposed to a mass or number density description) and use the stochastic methods of Part I to implement the chemical interactions. There are two main classes of algorithms that implement the chemical reactions of which the first one is the most popular. This first class are weight-updating schemes, the other class are called birth/death schemes since they manipulate the number of random walkers. Because of its popularity we will first derive a weight-updating scheme by combining a form of eq. (28) with a set of equations like eqs. (20). However, it is advisable not to use this scheme. The reason will become clear from the introduction to an algorithm of the second class. Since the interactions can change the identity of the molecules of a substance and thereby changing the total mass of that substance present in V , we expect the interactions to change the weight of the walkers. Therefore we should write eq.(28) as follows

$$\bar{C}(\vec{r}, t) = \sum_{j=1}^{N_s} \left(\sum_{\kappa=1}^{n_j(t)} w_{\kappa} \right) \delta(\vec{r} - \vec{r}_j) \quad (30)$$

Filling in eq.(30) for all substances in eqs.(20), one can show that one will get the following update scheme for all the weights associated with substance s

$$\begin{aligned} \frac{d}{dt} \left(\sum_{\kappa=1}^{n_s(t)} w_{s\kappa}(t) \right) &= f_s(\bar{C}_1(\vec{r}_s, t), \bar{C}_2(\vec{r}_s, t), \dots, \bar{C}_N(\vec{r}_s, t)) \quad \forall \kappa : \vec{r}_s \in \Delta V_s \\ \sum_{\kappa=1}^{n_s(t)} \frac{dw_{s\kappa}(t)}{dt} &= \sum_{i=1}^N K_{s,i} \prod_{j=1}^N \left(\sum_{\kappa=1}^{n_j(t)} w_{j\kappa}(t) \right)^{\nu_{ij}} \end{aligned} \quad (31)$$

where, in the second set of equations, we used the normal form for the f_s 's (eq.(19)). (The diffusional parts are handled by the random walks and make the nl time-dependent.) Generally, this means solving $N_w(s)$ coupled

nonlinear ODE's for every substance s , amounting to $\sum_{s=1}^N N_{w(s)}$ equations in total for every time step. When the f_s 's are linear in $\bar{C}_s(\vec{r}, t)$, the equations

become as follows :

$$\frac{dw_{s,\kappa}(t)}{dt} = f_s(\bar{C}_1(\vec{r}_s, t), \dots, \bar{C}_{s-1}(\vec{r}_s, t), \bar{C}_{s+1}(\vec{r}_s, t), \dots, \bar{C}_s(\vec{r}_s, t)) w_{s,\kappa}(t) \quad \kappa : 1, \dots, n_{s,\kappa} \quad (32)$$

with formal solution

$$w_{s,\kappa}(t + \Delta t) = w_{s,\kappa}(t) \exp\left(\int_t^{t+\Delta t} f_s d\tau\right) \approx w_{s,\kappa}(t) \exp(f_{s,\kappa} \Delta t) \quad (33)$$

where the approximation is assumed valid when the integrandum can be considered (nearly) constant in $]t, t+\Delta t[$. This update scheme guarantees positive weight values for positive initial values. Also, at a fixed position, the same exponential factor can be used for all the walkers corresponding to the same substance, providing a significant optimisation. The accuracy and stability of the solution will depend on the problem at hand, especially the degree of stiffness will be very important.

The term stiffness is generally used in the context of a coupled system of equations. It is a measure for the range of time scales in the simultaneous solutions of the equations. If one is interested in the fast time scales, it implies that one will lose a lot of time calculating the slowly changing components. If one is only interested in the slow components, it means that one runs the risk of numerical instability. Therefore special numerical algorithms should be applied to solve stiff systems. Runge-Kutta-Fehlberg with Rosenbrock-type extensions are simple and robust examples of such algorithms (see for example (Press *et al.*, 1992)).

Sometimes the term 'stiffness' is also used in the context of certain PDE's. In this case it means that the spatial and temporal scale are linked by a relation like eq.(5). However, in most cases one is interested in longer time scales for a fixed spatial scale than is prescribed by this relation. So, again, one is confronted with the dilemma of efficiency vs. numerical stability. Therefore also in this case one should use numerical algorithms specially suited for these equations (for example the implicit schemes as described in section 14).

Since the weights can change, nothing can stop them from becoming zero or very big. Walkers with zero (or arbitrary subthreshold) weights don't contribute (much) to the distribution function. Generating random walks for them is a waste of computation time. A popular practice is to disregard these small weight walkers all together (and possibly reuse their datastructures for redistributing large weight walkers, as described next). In case the weights become very large, they can cause instability, excessive variance and huge numerical errors. Therefore one could divide a walker with a large weight into smaller pieces. There are other methods to increase efficiency and reduce

variance but they depend on the specifics (like relative time scales) of the problem at hand. Without these weight control mechanisms, however, weight-update schemes tend to be very inefficient and produce results with large variances.

Sherman and Mascagni (Sherman and Mascagni, 1994) developed a similar method, called Gradient Random Walk (GRW). Instead of calculating the solution directly, it calculates the gradient of the solution. Their work is a good source of references to other particle methods to solve reaction-diffusion equations and to the mathematical foundations and computational properties of particle methods in general.

When using the combination of weight control mechanisms as described above, an important principle of MC simulations is violated. This 'correspondence principle' leads to the condition of 'detailed balance' [16] at thermodynamic equilibrium. It guarantees global balance (at thermodynamic equilibrium) and meaningful, consistent statistics (in general). A prerequisite for the correspondence principle to be met is to *preserve* the close correspondence-hence the name "correspondence principle"-between *local* changes in the distribution of random walkers and the *physical* processes that cause these local changes. This means that local reshuffling of random walkers for performance reasons is out of the question. Algorithms of the second class, however, meet this principle in an efficient manner when correctly implemented.

Deriving a particular scheme for second class algorithms starts from eq.(29) instead of eq. (28) : instead of making the weights dependent on time, like in eq.(30), one can find a scheme for changing the number $n_i(t)$ while keeping w_s fixed (on a per substance basis). By filling in eq. (29) in eqs.(20) one gets for every position \vec{r}_i :

$$\begin{aligned}
 w_s \frac{dn_{i,s}(t)}{dt} &= \sum_{c=1}^S K_{s,c} \prod_{f=1}^S (w_f n_{i,f}(t))^{v_{fc}} \\
 \frac{dn_{i,s}(t)}{dt} &= \sum_{c=1}^S \frac{K_{s,c}}{w_s} \prod_{f=1}^S w_f^{v_{fc}} \prod_{f=1}^S n_{i,f}^{v_{fc}}(t) \\
 &= \sum_{c=1}^S \Lambda_{s,c} \prod_{f=1}^S n_{i,f}^{v_{fc}}(t)
 \end{aligned} \tag{34}$$

(now with $\Lambda_{s,c} = (K_{s,c}/w_s) \prod_{f=1}^S w_f^{v_{fc}} = (k_c(v_{s,c}^R - v_{s,c}^L)/w_s) \prod_{f=1}^S w_f^{v_{fc}}$ which can be pre-computed). Now one only has to solve $N \ll N_{w(s)}(t)$

coupled nonlinear ODE's for every position \vec{r}_i that is occupied (by at least one substance), in the worst case scenario leading to at most

$$\sum_{s=1}^S N_{w(s)}(t) \left(= \sum_{s=1}^S N_{w(s)}(0) \right) \text{ sets of } N \text{ coupled equations of which most}$$

are trivial (i.e. zero change). Integrating this set of equations over Δt gives a change in the number of random walkers $\Delta n_{i,s}(t) (= n_{i,s}(t+\Delta t) - n_{i,s}(t))$ at position. Generally, $\Delta n_{i,s}(t)$ is not an integer, therefore one uses the

following rule : [17] create/destroy $\lfloor \Delta n_{i,s}(t) \rfloor$ random walkers and create/destroy an extra random walker with probability $\text{frac}(\Delta n_{i,s}(t))$. Note that now $N_w = R_i n_i(t)$ is not preserved! The correspondence principle is still met when globally scaling down the number of random walkers (and as a compensation renormalise their weight) for a substance in case their number has grown out of band due to nonFickian fluxes.

Now that one can select a method to incorporate chemical interactions, it has to be combined with the discrete random walk generator for diffusion. To simplify the implementation, one chooses a common spatial grid for all substances. Since for diffusion the temporal scale is intrinsically related to the spatial scale (by eq.(5)), this means a different Δt for every unique D . The simulation clock ticks with the minimal Δt , Δt_{\min} . Every clock tick, the system of eqs.(34) is solved to change the numbers of random walkers. Then a diffusion step should be performed for every substance s for which an interval Δt_s has passed since its last diffusion update at time t_s . Here we made the following implicit assumptions : the concentration of substance s in ΔV_i is assumed not to change due to diffusion during a time interval Δt_s and all substances are assumed to be well-mixed in every ΔV_i . The assumptions are justified if one chooses $\text{vol}(\Delta V_i)$ in such a way that in every ΔV_i the concentration changes every time step with atmost 10% for the fastest diffusing substance(s) (i.e. the one(s) with $\Delta t_s = \Delta t_{\min}$).

3.4 Discretization in space and time.

For a large enough number of molecules, it is sufficient to integrate the diffusion equations directly using for instance discretisation methods. Their scaling properties are much better (although, for multi-dimensional problems this is questionable) and, theoretically, they are also much faster. However, as can be seen from the equations (see below), their implementation can become more and more cumbersome for every additional interaction term and for growing geometrical complexity. So, although these methods are very popular because of their perceived superior performance, it's sometimes more feasible to use the Green's Function MC method (or another equivalent particle method) as a compromise between performance and ease of implementation.

The Crank-Nicholson method is an example of a classical implicit finite difference discretisation method that is very suited for diffusion problems. Section 15 introduces the formulation for one-dimensional (reaction-) diffusion and section 16 provides ADI, an extension to Crank-Nicholson to solve multi-dimensional problems.

3.5 One-dimensional diffusion.

Because the diffusion equation (eq.(6)) is a parabolic PDE-which makes it very stiff for most spatial scales of interest (Carnevale, 1989; Press *et al.*,

1992)-its solution prefers an implicit [18] solution method and its numerical solution is sensitive to the accuracy of the boundary conditions (Fletcher, 1991). For the discretisation, the volume will be split in a number of elements and the concentration is computed in each of them. This approximation for a real concentration will be good if sufficient molecules are present in each element so that the law of large numbers applies. This implies that the elements should not be too small, though this may of course lead to a loss of accuracy in representing gradients. The problem is not trivial. Take, for example, the calcium concentration in a dendritic spine (Koch and Zador, 1993). A resting concentration of 50 nM corresponds to exactly two calcium ions in the volume of a 0.5 μm diameter sphere, which is about the size of a spine head! The random walk methods described in the previous sections seem more appropriate for this situation. A popular assumption is that of a spherical cell where diffusion is modeled using the spherical radial equation (2nd eq. of eqs.(16)). The discretisation is performed by subdividing the cell into a series of onion shells with a uniform thickness of about 0.1 μm (Blumenfeld *et al.*, 1992) and figs.3-5). The Crank-Nicolson method is then the preferred solution method for finding the concentration in each shell after every time step Δt (Fletcher, 1991; Press *et al.*, 1992) as it is unconditionally stable and second order accurate in both space and time. We will continue using our example of calcium diffusion, which leads to a set of difference equations of the form:

$$\begin{aligned}
& -\frac{\Delta t}{2} D_{Ca} C_{i-1,i} [Ca^{2+}]_{i-1,i+\Delta t} + \left(1 + \frac{\Delta t}{2} D_{Ca} (C_{i-1,i} + C_{i,i+1}) \right) [Ca^{2+}]_{i,i+\Delta t} \\
& \quad - \frac{\Delta t}{2} D_{Ca} C_{i+1,i} [Ca^{2+}]_{i+1,i+\Delta t} \\
& = \frac{\Delta t}{2} D_{Ca} C_{i-1,i} [Ca^{2+}]_{i-1,i} + \left(1 - \frac{\Delta t}{2} D_{Ca} (C_{i-1,i} + C_{i,i+1}) \right) [Ca^{2+}]_{i,i} \\
& \quad + \frac{\Delta t}{2} D_{Ca} C_{i+1,i} [Ca^{2+}]_{i+1,i}
\end{aligned} \tag{35}$$

Note that the equations express the unknown $([Ca^{2+}]_{i,i+\Delta t})$ in terms of the knowns (the right-hand side terms) but also of the unknowns for the neighboring shells. Therefore, this requires an iterative solution of the equations, which is typical for an implicit method. The terms containing $i+1$ are absent in the outer shell $i=n$ and those containing $i-1$ in the innermost shell $i=0$. This system of equations can be applied to any one-dimensional morphology, where the geometry of the problem is described by the coupling constants $C_{i,i+1}$. In the case of a spherical cell the coupling constants are of the form :

$$C_{i,t+1} = \frac{3(i+1)^2}{(3i^2 + 3i + 1)\Delta r^2} \quad (36)$$

where Δr is the uniform thickness of the shells and the diameter of the cell is equal to $d=2n\Delta r$. See De Schutter and Smolen (1998) for practical advise on how to apply these equations to more complex geometries.

The system of algebraic equations eqs.(35) can be solved very efficiently because its corresponding matrix is tridiagonal with diagonal dominance (Press *et al.*, 1992). Influx across the plasma membrane can be simulated by

adding a term $(\Delta t/2)(J_{\text{in}} + \Delta t/2 / v_{\text{in}})$ to the right-hand side of the equation corresponding to the outer shell. Computing the flux at $t+\Delta t/2$ maintains the second order accuracy in time (Mascagni and Sherman, 1998). Note that the overall accuracy of the solution will depend on how exactly this boundary condition J_{in} is met (Fletcher, 1991).

In the case of buffered diffusion the buffer reaction eq.(22) has to be combined with eqs.(35). This leads to a new set of equations with for every shell one equation for each diffusible buffer:

$$\begin{aligned} & -\frac{\Delta t}{2} D_B C_{i-1,t} [B]_{i-1,t+\Delta t} - \frac{\Delta t}{2} D_B C_{i,t+1} [B]_{i+1,t+\Delta t} \\ & + \left(1 + \frac{\Delta t}{2} \left(D_B (C_{i-1,t} + C_{i,t+1}) + b + f[C_{\text{Ca}}^{2+}]_{i,t} \right) \right) [B]_{i,t+\Delta t} \\ & = \frac{\Delta t}{2} D_B C_{i-1,t} [B]_{i-1,t} + \frac{\Delta t}{2} D_B C_{i,t+1} [B]_{i+1,t} \\ & + \left(1 - \frac{\Delta t}{2} \left(D_B (C_{i-1,t} + C_{i,t+1}) + b \right) \right) [B]_{i,t} + \Delta t b [B]_{T,t} \end{aligned} \quad (37)$$

and an equation for buffered calcium diffusion:

$$\begin{aligned} & -\frac{\Delta t}{2} D_{\text{Ca}} C_{i-1,t} [C_{\text{Ca}}^{2+}]_{i-1,t+\Delta t} - \frac{\Delta t}{2} D_{\text{Ca}} C_{i,t+1} [C_{\text{Ca}}^{2+}]_{i+1,t+\Delta t} \\ & + \left(1 + \frac{\Delta t}{2} \left(D_{\text{Ca}} (C_{i-1,t} + C_{i,t+1}) + f[B]_{i,t} \right) \right) [C_{\text{Ca}}^{2+}]_{i,t+\Delta t} \\ & = \frac{\Delta t}{2} D_{\text{Ca}} C_{i-1,t} [C_{\text{Ca}}^{2+}]_{i-1,t} + \frac{\Delta t}{2} D_{\text{Ca}} C_{i,t+1} [C_{\text{Ca}}^{2+}]_{i+1,t} \\ & + \left(1 - \frac{\Delta t}{2} D_{\text{Ca}} (C_{i-1,t} + C_{i,t+1}) \right) [C_{\text{Ca}}^{2+}]_{i,t} + \Delta t b \left([B]_{T,t} - \frac{1}{2} [B]_{i,t} \right) \end{aligned} \quad (38)$$

Equation (38) applies to a system with only one buffer. In case of multiple

buffers, one additional term appears at the left-hand side and two at the right-hand side for each buffer. We have also assumed that DB is identical for the free and bound forms of the buffer, which gives a constant $[B]_{T,i}$. This is reasonable taking into account the relative sizes of calcium ions as compared to most buffer molecules.

Eqs.(37) and (38) should be solved simultaneously, resulting in a diagonally banded matrix with three bands for the calcium diffusion and two bands extra for each buffer included in the model.

3.6 Two-dimensional diffusion.

An elegant extension to the Crank-Nicholson method is the Alternating Direction Implicit (ADI) method which allows for an efficient solution of two-dimensional diffusion problems (Fletcher, 1991; Press *et al.*, 1992). Each time step is divided into two steps of size $\Delta t/2$ and in each substep the solution is computed in one dimension:

$$\begin{aligned}
 & -\frac{\Delta t}{4} D_{Ca} C_{i-1,j} [Ca^{2+}]_{i-1,j,t+\Delta t/2} + \left(1 + \frac{\Delta t}{4} D_{Ca} (C_{i-1,j} + C_{i,j+1})\right) [Ca^{2+}]_{i,j,t+\Delta t/2} \\
 & \quad - \frac{\Delta t}{4} D_{Ca} C_{i,j+1} [Ca^{2+}]_{i,j+1,t+\Delta t/2} \\
 & = \frac{\Delta t}{4} D_{Ca} C_{i-1,j} [Ca^{2+}]_{i-1,j,t} + \left(1 - \frac{\Delta t}{4} D_{Ca} (C_{i-1,j} + C_{i,j+1})\right) [Ca^{2+}]_{i,j,t} \\
 & \quad + \frac{\Delta t}{4} D_{Ca} C_{i,j+1} [Ca^{2+}]_{i,j+1,t}
 \end{aligned} \tag{39}$$

respectively

$$\begin{aligned}
 & -\frac{\Delta t}{4} D_{Ca} C_{j-1,i} [Ca^{2+}]_{i,j-1,t+\Delta t} + \left(1 + \frac{\Delta t}{4} D_{Ca} (C_{j-1,i} + C_{j,i+1})\right) [Ca^{2+}]_{i,j,t+\Delta t} \\
 & \quad - \frac{\Delta t}{4} D_{Ca} C_{j,i+1} [Ca^{2+}]_{i,j+1,t+\Delta t} \\
 & = \frac{\Delta t}{4} D_{Ca} C_{j-1,i} [Ca^{2+}]_{i,j-1,t+\Delta t/2} + \left(1 - \frac{\Delta t}{4} D_{Ca} (C_{j-1,i} + C_{j,i+1})\right) [Ca^{2+}]_{i,j,t+\Delta t/2} \\
 & \quad + \frac{\Delta t}{4} D_{Ca} C_{j,i+1} [Ca^{2+}]_{i,j+1,t+\Delta t/2}
 \end{aligned} \tag{40}$$

where first diffusion along the i dimension is solved implicitly and then over the j dimension. The coupling constants $C_{i,i+1}$ and $C_{j,j+1}$ again depend on the geometry of the problem and are identical and constant in the case of a square grid. The two matrices of coupled equations (39) and (40) are tridiagonal with diagonal dominance and can be solved very efficiently. In

two dimensions, the ADI method is unconditionally stable for the complete time step and second order accurate in both space and time, provided the appropriate boundary conditions are used (Fletcher, 1991). Holmes (Holmes, 1995) used the two-dimensional ADI method with cylindrical coordinates to model glutamate diffusion in the synaptic cleft. The ADI method can also be applied to simulate three-dimensional diffusion with substeps of $\Delta t/3$, but in this case it is only conditionally stable (Fletcher, 1991).

4. Case study.

In general, we're interested in compartmental models of neurons using detailed reconstructed morphologies, in particular of the dendritic tree. These compartments are cylindrical idealisations of consecutive tubular sections of dendritic membrane. Because of the cylindrical nature of the compartments we prefer a description in cylindrical coordinates, giving us an accurate representation of the concentration in the submembrane region. This is important for a number of our other simulations. As can be seen from eq.(15), using cylindrical coordinates introduces factors depending on $1/\rho$ and an additional first-order term in ρ . These are pure geometric effects and arise from the fact that an infinitesimal volume element in cylindrical coordinates is of the form $dV = \rho d\rho d\phi dz$ which is dependent on ρ .

Just like in the 1D case, eq.(11)(2nd eq.) can be derived from a (discrete) random walk process. That is, in Cartesian coordinates, for every second order term on the right-hand side of eq. (11)(2nd eq.) the corresponding coordinate of the random walker's position is updated according to the 1D random walk scheme. However, this recipe does not work when writing out a random walk scheme for eq.(14) due to the extra first-order term. A more general recipe for deriving the appropriate random walk process can be obtained by considering more closely the consequences of the ρ - dependency of dV .

In order to maintain a uniform distribution of mass at equilibrium, there should be less mass in the volume elements closer to the origin, since for smaller ρ , i.e. nearer to the origin, the volume elements get smaller. Therefore the random walkers (which correspond to mass units) should tend to step more often away from the origin than toward the origin when equilibrating, creating a net drift outward. Eventually, in a closed volume with reflecting walls this drift will come to a halt at equilibrium, while the outward tendency creates a gradient in ρ in the number (but not density!) of walkers. The tendency is introduced by adjusting the probability to choose the direction of a ρ -step.

The adjustment is derived as follows for a drifting 1D random walk : suppose the walkers have a drift speed c (negative to go to the left, positive to go to the right) then the probability to go to the left is

$$\begin{cases} p_l &= \frac{1}{2} \left(1 - \frac{c\Delta t}{\Delta x} \right) \\ p_r = 1 - p_l &= \frac{1}{2} \left(1 + \frac{c\Delta t}{\Delta x} \right) \end{cases} \quad (0 \leq p_l, p_r \leq 1) \quad (41)$$

(with obvious conditions on Δt and Δx for a given c). When filling in these expressions for $p_{l,r}$ in eq.(1) and taking the appropriate limits, one gets the following equation

$$\frac{\partial C(x,t)}{\partial t} = D \frac{\partial^2 C(x,t)}{\partial x^2} + c \frac{\partial C(x,t)}{\partial x} \quad (42)$$

Note the correspondence between this equation and the radial part of eq. (14). Therefore we extend the recipe as follows : every first-order term corresponds to a drift with the drift speed c given by the coefficient of the partial derivative and the probabilities are adjusted according to eq.(41). If we ignore the $1/\rho$ factors by defining new 'constants' $c=D/r$ and $D'=D/r^2$, we get the following random walk scheme in cylindrical coordinates : for every time step $t \rightarrow t+\Delta t$, for every walker k ($1 \leq k \leq N_w$) the following coordinate update is performed :

$$\begin{cases} r_x(t) = k\Delta r & \rightarrow & r_x(t+\Delta t) = (k \pm 1)\Delta r & (k \in \mathbb{N}) \\ \phi_x(t) & \rightarrow & \phi_x(t+\Delta t) = \phi_x(t) \pm \Delta\phi(r) \\ z_x(t) = l\Delta z & \rightarrow & z_x(t+\Delta t) = (l \pm 1)\Delta z & (l \in \mathbb{N}) \end{cases} \quad (43)$$

where we choose

$$\begin{cases} (\Delta r)^2 = (\Delta z)^2 = 2D\Delta t \\ (\Delta\phi(r))^2 = 2D'\Delta t = \left(\frac{\Delta r}{r} \right)^2 = \frac{1}{k^2} \quad (k > 0) \end{cases} \quad (44)$$

with the following probabilities for the respective signs :

$$\begin{cases} p_{\pm}^r &= \frac{1}{2} \left(1 \pm \frac{c\Delta t}{\Delta r} \right) = \frac{1}{2} \left(1 \pm \frac{1}{2k} \right) \quad k > 0 \\ p_{\pm}^{\phi} = p_{\pm}^z &= \frac{1}{2} \end{cases} \quad (45)$$

and $(p_{-}^r=0, p_{+}^r=1)$ for $k=0$. This type of random walk is called a Bessel walk.

From the $1/r^n$ factors in the diffusion equation one expects problems of divergence in the origin. The way we handle the random walks in the origin (i.e. for $k=0$) seems to work fine as can be seen from simulation results. Of course, due to the low number of walkers in the origin, the variance is quite large in the region around the origin.

The discrete natures of the geometry and the random walk introduce other specific problems, among which are connections of compartments with different radii, branchpoints and regions of spine neck attachments to the compartmental mantle. We used minimalistic approaches to these problems by using probabilistic models. Concerning the connections for example, we assigned a probability for the transition that the random walker could make between two connected cylinders in such a way that p_{\pm}^z becomes

$$p_{\pm}^z = \begin{cases} \frac{1}{2} & R_1 \leq R_2 \\ \frac{1}{2} \left(1 - \left(\frac{R_2}{R_1} \right)^2 \right) & R_1 > R_2 \end{cases} \quad (46)$$

(where the sign is chosen in accordance with the end of the cylinder at which the walker is) in case the walker is at the end of cylinder 1 that is connected to cylinder 2. When the walker makes the transition to cylinder 2, its ρ -coordinate is adjusted according to $\rho_{\text{new}} = (R_2/R_1) \rho_{\text{old}}$. This way no artificial gradients are created in the area around the discrete transition. Instead, the walkers behave more like walkers in a tapered cylinder, which is the more natural geometry for dendritic branches.

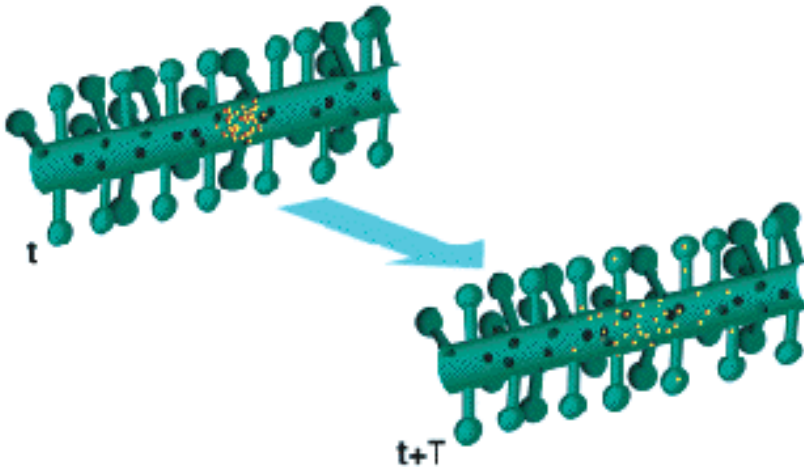


Figure 6

The effect of the presence of spines on the longitudinal component of diffusion in the dendritic shaft. Compare with fig.1 for the smooth case (i.e. without spines). The yellow dots represent (small sphere-like) molecules. In the model, the spine heads-the small spheres on the spine necks shown here as sticks perpendicular to the dendritic

shaft-are modeled as short, wide cylinders.

Recent caged compound release experiments in neuronal spiny dendrites (Wang and Augustine, 1995) and (Bormann *et al.*, 1997) show a slowing in the apparent diffusion (see fig.6). The apparent diffusion constant is defined as the diffusion constant for the effective 1D diffusion along the longitudinal axis of the dendritic shaft. The experiments were performed with both relatively inert and highly regulated substances. We were interested in estimating the contribution of geometric factors to this slowing in apparent diffusion rate, especially the effect of 'hidden' volume (mostly spines) and morphology (branching, structures in cytoplasm).

In order to isolate the contributing factors, we constructed simple geometrical models of dendritic structures including spines and single branchpoints. Then we simulated idealised release experiments by using square pulses as initial condition and calculated the apparent diffusion coefficient $D_{app}(t)$ from the resulting concentration profiles as follows :

$$D_{app}(t) = \frac{\langle z^2 \rangle(t) - \langle z^2 \rangle(0)}{2t} \quad (47)$$

with

$$\langle z^2 \rangle(t) = \int_{-\infty}^{+\infty} (z - \langle z \rangle)^2 C(z, t) dz \quad (48)$$

The integral is cut off at the endpoints of the (chain of consecutive) cylinders, which is ok when the distance between the endpoints is large enough so that only very few walkers will arrive at either of the endpoints in the simulated time period. The simulator is instructed to output

$C(z, t) = \overline{C(\rho, \phi, z, t)}^{(\rho, \phi)}$, i.e. the ρ - and ϕ -dependence is averaged out.

Slowing is expressed by a slowing factor $\lambda(t)$, defined as

$\lambda(t) = D_{app}(t) / D \leq 1.0 \quad \forall t \geq 0$. The apparent diffusion constant D_{app} at equilibrium is defined as $D_{app} = D_{app}(t \rightarrow \infty)$.

Fig.7 shows the difference in time evolution of two concentration profiles. One is for a smooth dendrite (modeled as a simple cylinder), the other for a spiny dendrite of the same length but with spines distributed over its plasma membrane. The spines are attached perpendicularly on the cylindrical surface and consist of 2 cylinders : one narrow for the neck (attached to the surface) and one wide for the head. The figure shows the results for the most common spines parameters (density, neck and head lengths and radii) on Purkinje cell dendrites.

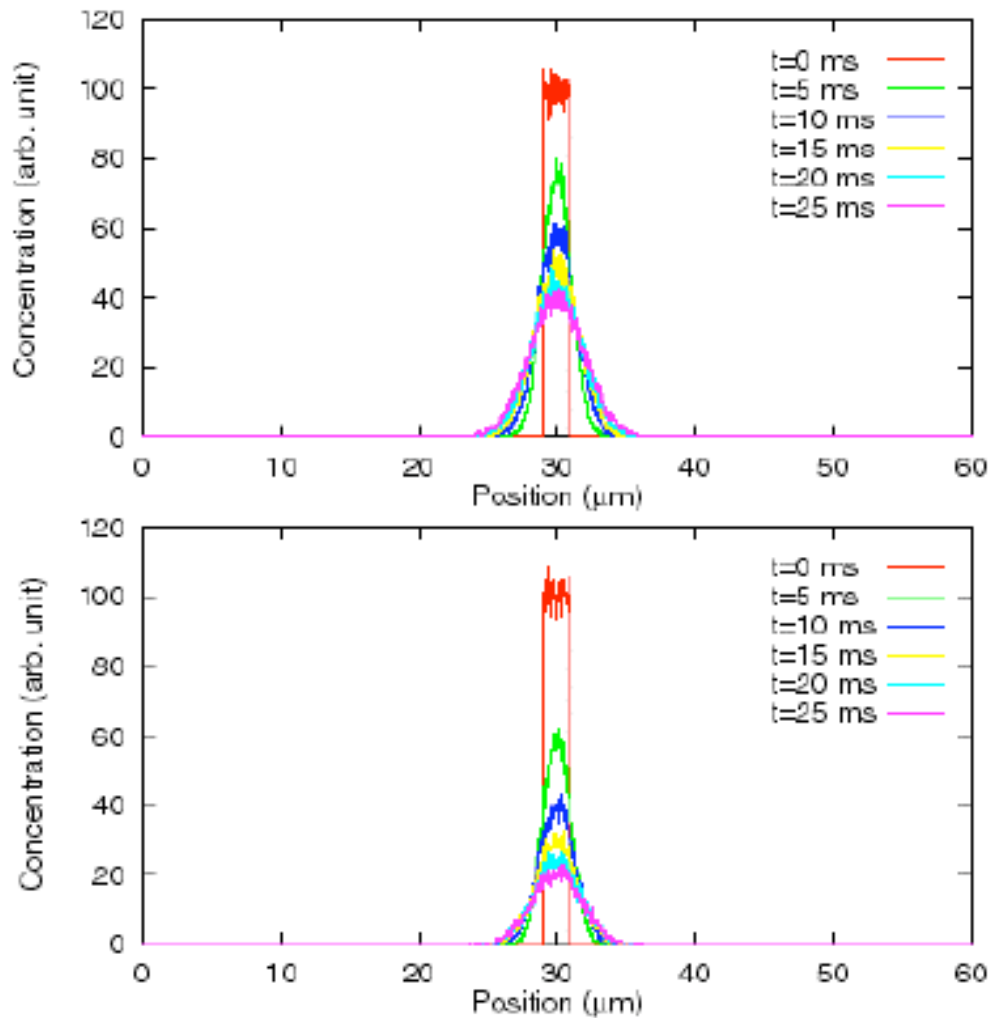


Figure 7

Concentration profiles along length axis of the dendritic shaft.

Upper frame : Smooth dendrite case (see text).

Lower frame : Spiny dendrite case (see text).

The corresponding $\lambda(t)$ curves can be found, overlapped, in fig.8. The small amount of slowing in the smooth dendrite case is due to reflection at the endpoints, which is neglectable for the period of simulation time used. We found $\lambda(0)/\lambda(\infty)$'s of 1.0-3.0 for various geometric parameters of the spines. (We used $\lambda(0)/\lambda(\infty)$ to express total slowing instead of $\lambda^{-1}(\infty)$ because $D_{app}(0)$ is only equal to D for initial conditions that are solution of the diffusion equation.)

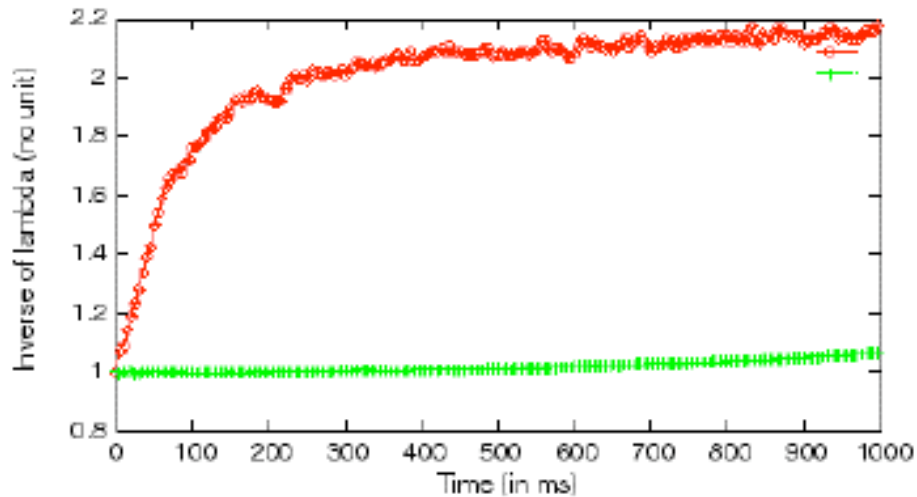


Figure 8

Slowing factor curves.

Red curve Spiny dendrite case (see text).

Blue curve Smooth dendrite case (see text).

5 Conclusion.

In this chapter we have demonstrated that diffusional processes can dominate the kinetics of molecular processes. Moreover, in many cases the effect of diffusion is strongly influenced by the boundary conditions, in particular by the local geometry of the cell in all three dimensions. However, most models of reaction-diffusion systems to date have assumed some form of spatial symmetry so that they could be reduced to a one-dimensional system. As a consequence, efficient methods to simulate three-dimensional reaction-diffusion systems are still under development.

References

- Albritton ML, Meyer T, Stryer L (1992) Range of messenger action of calcium ion and inositol 1,4,5-triphosphate. *Science* 258:1812-1815.
- Augustine GJ, Charlton MP, Smith SJ (1985) Calcium entry and transmitter release at voltage-clamped nerve terminals of squid. *J Physiol* 367:163-181.
- Baimbridge KG, Celio MR, Rogers JH (1992) Calcium-binding proteins in the nervous system. *Trends Neurosci* 15:303-308.
- Bartol TM, Land br, Salpeter EE, Salpeter MM (1991) Monte Carlo simulation of miniature end-plate current generation in the vertebrate neuromuscular junction. *Biophys J* 59:1290-1307.
- Bartol TMJ, Stiles JR, Salpeter MM, Salpeter EE, Sejnowski TJ (1996) MCELL: Generalised Monte Carlo computer simulation of synaptic transmission and chemical signaling. *Abstr Soc Neurosci* 22:1742.
- Berridge MJ (1997) The AM and FM of calcium signaling. *Nature* 386:759-760.
- Bezprozvanny I (1994) Theoretical analysis of calcium wave propagation based on inositol (1,4,5)-triphosphate (InsP3) receptor functional properties. *Cell Calcium* 16:151-166.
- Bezprozvanny I, Watras J, Ehrlich BE (1991) Bell-shaped calcium-dependent curves of Ins(1,4,5)P3-gated and calcium-gated channels from endoplasmic

reticulum of cerebellum. *Nature* 351:751-754.

Blumenfeld H, Zablow L, Sabatini B (1992) Evaluation of cellular mechanisms for modulation of calcium transients using a mathematical model of fura-2 Ca²⁺ imaging in *Aplysia* sensory neurons. *Biophys J* 63:1146-1164.

Bormann G, Wang SS-H, De Schutter E, Augustine GJ (1997) Impeded diffusion in spiny dendrites of cerebellar Purkinje cells. *Abstr Soc Neurosci* 23:2008.

Bower JM, Beeman D. (1995). *The book of GENESIS: exploring realistic neural models with the GEneral NEural Simulation System*. New York, NY: TELOS.

Carnevale NT (1989) Modeling intracellular ion diffusion. *Abstr Soc Neurosci* 15:1143.

Crank J. (1975). *The mathematics of diffusion*. Oxford, U.K.: Clarendon Press.

De Raedt H, von der Linden W. (1995). *The MC method in condensed matter physics*. (2nd Ed. ed.). (Vol. 71). Berlin: Springer-Verlag.

[De Schutter E, Smolen P.](#) (1998). Calcium dynamics in large neuronal models. In: *Methods in neuronal modeling: from ions to networks* (Koch C & Segev I, ed. eds.) (2nd ed.,), pp. 211-250. Cambridge, MA: MIT Press.

DiFrancesco D, Noble D (1985) A model of cardiac electrical activity incorporating ionic pumps and concentration changes. *Phil Trans Roy Soc London Ser B* 307:353-398.

Dolmetsch RE, Xu K, Lewis RS (1998) Calcium oscillations increase the efficiency and specificity of gene expression. *Nature* 392:933-936.

Einstein A (1905) On the movement of small particles suspended in a stationary liquid demanded by the molecular kinetics of heat. *Ann Phys* 17:549-560.

Exton JH (1997) Phospholipase D: enzymology, mechanisms of regulation, and function. *Physiol Rev* 77:303-320.

Farnsworth CL, Freshney NW, Rosen LB, Ghosh A, Greenberg ME, Feig LA (1995) Calcium activation of Ras mediated by neuronal exchange factor Ras-GRF. *Nature* 376:524-527.

Feynman RP, Leighton RB, Sands M. (1989). *The Feynman Lectures on Physics (Commemorative Issue)*: Addison-Wesley.

Fick A (1885) Ueber Diffusion. *Ann Phys Chem* 94:59-86.

Fishman GS. (1996). *Monte Carlo : Concepts, Algorithms and applications.*: Springer-Verlag.

Fletcher CAJ. (1991). *Computational techniques for fluid dynamics*. Volume I. Berlin: Springer-Verlag.

Foley J, Van Dam A, Feiner S, Hughes J. (1990). *Computer graphics : principles and practice*. (2nd ed.): Addison-Wesley.

Garrahan PJ, Rega AF. (1990). Plasma membrane calcium pump. In: *Intracellular calcium regulation* (Bronner F, ed. eds.) , pp. 271-303. New York: Alan R. Liss.

Gola M, Crest M (1993) Colocalization of active KCa channels and Ca²⁺ channels within Ca²⁺ domains in *Helix* neurons. *Neuron* 10:689-699.

Goldbeter A, Dupont G, Berridge MJ (1990) Minimal model for signal-induced Ca^{2+} oscillations and for their frequency encoding through protein phosphorylation. *Proc Natl Acad Sci USA* 87:1461-1465.

Hille B. (1992). Ionic channels of excitable membranes. Sunderland: Sinauer Associates.

Holmes WR (1995) Modeling the effect of glutamate diffusion and uptake on NMDA and non-NMDA receptor saturation. *Biophys J* 69:1734-1747.

Issa NP, Hudspeth AJ (1994) Clustering of Ca^{2+} channels and Ca^{2+} -activated K^+ channels at fluorescently labeled presynaptic active zones of hair cells. *Proc Natl Acad Sci USA* 91:7578-7582.

Jafri SM, Keizer J (1995) On the roles of Ca^{2+} diffusion, Ca^{2+} buffers, and the endoplasmic reticulum in IP_3 -induced Ca^{2+} waves. *Biophys J* 69:2139-2153.

Kasai H, Petersen OH (1994) Spatial dynamics of second messengers: IP_3 and cAMP as long-range and associative messengers. *Trends Neurosci* 17:95-101.

Koch C, Zador A (1993) The function of dendritic spines: devices subverting biochemical rather than electrical compartmentalization. *J Neurosci* 13:413-422.

Li W, Llopis J, Whitney M, Zlokarnik G, Tsien RY (1998) Cell-permeant caged InsP_3 ester shows that Ca^{2+} spike frequency can optimize gene expression. *Nature* 392:936-941.

Linse S, Helmersson A, Forsen S (1991) Calcium-binding to calmodulin and its globular domains. *J Biol Chem* 266:8050-8054.

Llano I, DiPolo R, Marty A (1994) Calcium-induced calcium release in cerebellar Purkinje cells. *Neuron* 12:663-673.

Llinás RR, Sugimori M, Silver RB (1992) Microdomains of high calcium concentration in a presynaptic terminal. *Science* 256:677-679.

Mahama PA, Linderman JJ (1994) A Monte Carlo study of the dynamics of G-protein activation. *Biophys J* 67:1345-1357.

Markram H, Roth A, Helmchen F (1998) Competitive calcium binding: implications for dendritic calcium signaling. *J Comput Neurosci* 5:331-348.

Mascagni MV, Sherman AS. (1998). Numerical methods for neuronal modeling. In: *Methods in neuronal modeling: from ions to networks* (Koch C & Segev I, ed. eds.) (2nd ed.,), pp. 569-606. Cambridge, MA: MIT Press.

Naraghi M, Neher E (1997) Linearized buffered Ca^{2+} diffusion in microdomains and its implications for calculation of $[\text{Ca}^{2+}]$ at the mouth of a calcium channel. *J Neurosci* 17:6961-6973.

Nixon RA (1998) The slow axonal transport of cytoskeletal proteins. *Curr Opin Cell Biol* 10:87-92.

Nowycky MC, Pinter MJ (1993) Time courses of calcium and calcium-bound buffers following calcium influx in a model cell. *Biophys J* 64:77-91.

Press WH, Teukolsky SA, Vetterling WT, Flannery BP. (1992). *Numerical recipes in C: The art of scientific computing*. (2nd ed.). Cambridge: Cambridge University Press.

Qian N, Sejnowski TJ (1990) When is an inhibitory synapse effective? Proc Natl Acad Sci USA 87:8145-8149.

Regehr WG, Atluri PP (1995) Calcium transients in cerebellar granule cell presynaptic terminals. Biophys J 68:2156-2170.

Sala F, Hernandez-Cruz A (1990) Calcium diffusion modeling in a spherical neuron: relevance of buffering properties. Biophys J 57:313-324.

Schulman LS. (1981). Techniques and applications of path integration. New York, N.Y.: John Wiley & Sons.

Sherman A, Mascagni M (1994) A gradient random walk method for two-dimensional reaction-diffusion equations. SIAM J Sci Comput 15:1280-1293.

Sneyd J, Charles AC, Sanderson MJ (1994) A model for the propagation of intracellular calcium waves. Amer J Physiol 266:C293-C302.

Sneyd J, Wetton BTR, Charles AC, Sanderson MJ (1995) Intercellular calcium waves mediated by diffusion of inositol triphosphate: a two-dimensional model. Amer J Physiol 268:C1537-C1545.

Wagner J, Keizer J (1994) Effects of rapid buffers on Ca^{2+} diffusion and Ca^{2+} oscillations. Biophys J 67:447-456.

Wahl LM, Pouzat C, Stratford KJ (1996) Monte Carlo simulation of fast excitatory synaptic transmission at a hippocampal synapse. J Neurophysiol 75:597-608.

Wang SS-H, Augustine GJ (1995) Confocal imaging and local photolysis of caged compounds: dual probes of synaptic function. Neuron 15:755-760.

Zador A, Koch C (1994) Linearized models of calcium dynamics: formal equivalence to the cable equation. J Neurosci 14:4705-4715.

Zhou Z, Neher E (1993) Mobile and immobile calcium buffers in bovine adrenal chromaffin cells. J Physiol 469:245-273.